Cambridge Centre for Computational Chemical Engineering

University of Cambridge

Department of Chemical Engineering

Preprint ISSN 1473 – 4273

Partially Stirred Reactor Model: Analytical Solutions and Numerical Convergence Study of PDF/Monte Carlo Method

Amit Bhave, Markus Kraft[1]

submitted: 16th July 2002

[1] Department of Chemical Engineering
University of Cambridge
Pembroke Street
Cambridge CB2 3RA
UK
E-Mail: ab349@cam.ac.uk
E-Mail: markus_kraft@cheng.cam.ac.uk

Preprint No. 7

c4e

Key words and phrases. Partially stirred reactor model; analytical solutions; PDF/Monte Carlo method; numerical convergence.

Edited by
Cambridge Centre for Computational Chemical Engineering
Department of Chemical Engineering
University of Cambridge
Cambridge CB2 3RA
United Kingdom.

Fax: + 44 (0)1223 334796
E-Mail: c4e@cheng.cam.ac.uk
World Wide Web: http://www.cheng.cam.ac.uk/c4e/

Abstract

Partially stirred reactor (PaSR), a stochastic reactor model based on a simplified joint composition PDF transport equation, is investigated numerically. Analytical solutions for the first four moments of the mass density function (MDF), for four different Cauchy problems obtained from the MDF transport equation are presented. The Monte Carlo particle method with first order time splitting algorithm is implemented to obtain the first four moments of the MDF numerically. The dynamics of the stochastic particle system is determined by inflow-outflow, reaction and mixing events. Three different inflow-outflow algorithms are investigated : algorithm based on the inflow-outflow event modelled as a poisson process; inflow-outflow algorithm mentioned in the literature and a novel algorithm derived on the basis of analytical solutions. It is demonstrated that the inflow-outflow algorithm used in the literature can be explained by considering a deterministic waiting time parameter of a corresponding stochastic process, and also forms a specific case of the new algorithm. The number of particles in the ensemble, N, the non-dimensional time step, Δt^*(ratio of the global time step to the characteristic time of an event), and the number of independent simulation trials, L are the three sources of the numerical error. Based on the split analytical solutions, the convergence with respect to Δt^* is studied. Numerical experiments are carried out to study the convergence with respect to N and L. For a linear reaction, and the IEM model implemented, the investigation reveals that the systematic error converges as N^{-1} and Δt^*. The statistical error scales as $L^{-1/2}$ and $N^{-1/2}$. Finally the significance of the numerical parameters and the inflow-outflow algorithms is studied, by applying the PaSR model to a practical case of premixed kerosene and air combustion.

Contents

1 Introduction

In many practical combustion devices, e.g., gas turbines, the characteristic time scales for mixing are of the same order of magnitude as the time scales for chemical kinetics. When modelling such practical combustion devices it is important to account for both effects. However in order to include detailed reaction chemistry, simplifying assumptions regarding the fluid flow description are necessary to avoid excessive computational and storage expenses. The partially stirred reactor (PaSR) is one such model based on the probability density function (PDF) transport equation of the physical quantities, assuming statistical spatial homogeneity. The model accounts for mixing and is computationally efficient for large coupled chemical reaction mechanisms involving many chemical species.

Several applications of the PaSR model are mentioned in the literature. An early example of the simulation of a stirred tank reactor incorporating mixing, through-flow and reaction, is given in [13]. Over the last decade, with the substantial improvement in data storage and computational power, PaSR has received increased attention in combustion research. PaSR model was employed to investigate premixed methane combustion and study the effect of mixing frequency on composition and temperature [6]. PaSR was applied to evaluate reduced chemistry mechanisms for hydrogen combustion, and compared with detailed chemistry mechanisms [5]. Cannon et al. [4] used three reduced mechanisms to investigate their performance in the prediction of CO and NO in premixed turbulent combustion of methane and air simulated in a PaSR. The PaSR model was used to study the coupling effect of chemistry and mixing for detailed and reduced chemical kinetics, and a projection scheme was introduced for mixing models to be used in conjunction with the intrinsic low dimensional manifold (ILDM) method [2]. Thus, PaSR offers an ideal test bed for evaluating reduced chemical mechanisms as well as mixing schemes, for use in PDF-methods-based models.

The PaSR model can be derived from the one point joint scalar PDF transport equation, assuming statistical homogeneity [5]. The analytical solutions for some simple cases of the PDF transport equation describing the PaSR model have been presented in [11]. The PDF equation has been solved numerically using a Monte Carlo particle method with time splitting techniques. This method involves approximating the PDF by an ensemble of stochastic particles, and has been successfully exploited for solving high dimensional PDF equations [8, 16, 17]. However, with the implementation of Monte Carlo particle techniques, a need for sufficiently small time step has been emphasised in previous works [6, 5, 4]. In order to remove the dependence of simulation on the time step, Chen [5] introduced an improved PaSR algorithm based on theoretical age distribution of particles. However, the effect of this modified algorithm on the resulting PDF transport equation is not clear.

To understand the influence of the numerical parameters in a numerical algorithm, a systematic investigation of the convergence of the algorithm is essential. Recently, in [18] a semi-analytic, steady state solution of the pdf for a PaSR model was

presented and compared with a numerical solution obtained using a standard Monte Carlo particle algorithm as mentioned in [6, 5]. Overall, in the context of PDF methods, Xu and Pope [19] noted that less attention has been paid to the accuracy of numerical algorithms. Particularly, the literature does not report convergence study of the Monte Carlo particle algorithms implemented for PaSR.

The *aims of the present work* are as follows:

- To extend and develop the analytical solutions presented in [11], to a more general case of the MDF transport equation and obtain the first four moments (zeroth to third) of the mass density function (MDF) describing the PaSR model.
- To present a novel inflow-outflow algorithm, derived on the basis of the analytical solution, and to compare its performance with that of the inflow-outflow algorithm mentioned in the literature, by implementing both in a Monte Carlo particle scheme with time splitting.
- Based on analytical solutions, understand the significance of the global time step in the time splitting scheme and study the convergence of the Monte Carlo particle method with respect to the various numerical parameters.

The paper is organised in the following way. The PaSR model is discussed and the analytical solutions for the MDF and its first four moments are presented in **Section 2**. In **Section 3**, we describe a Monte Carlo particle scheme based on particle approximation and a time splitting technique. Additionally the inflow-outflow algorithm based on a stochastic jump approach is described. A new inflow-outflow algorithm is derived based on the analytical solutions. These two inflow-outflow algorithms are compared with the inflow-outflow algorithm mentioned in the literature. **Section 4** is devoted to numerical experiments, dealing with the order of convergence of the particle algorithm with respect to particle ensemble size N, number of independent simulation trials L and the non dimensional time step Δt^* (ratio of time step to the characteristic time of an event). In **Section 5**, a practical case of premixed kerosene and air combustion is studied using the PaSR model. Conclusions are drawn in **Section 6**.

2 PaSR model and analytical solutions

The PaSR model is described by the following PDE, giving the evolution of the joint composition MDF:

$$\frac{\partial \mathcal{F}(\psi,t)}{\partial t} + \sum_{l=1}^{R+1} \frac{\partial}{\partial \psi_l}\Big[\big(A_l(\psi) + S_l(\psi)\big)\mathcal{F}(\psi,t)\Big] = \frac{1}{\tau}\left(\mathcal{F}_{in}(\psi) - \mathcal{F}(\psi,t)\right) \tag{1}$$

with the initial conditions,

$$\mathcal{F}(\psi;0) = \mathcal{F}_0(\psi). \tag{2}$$

The MDF is represented by $\mathcal{F}$, and the variable ψ represents scalars such as mass fraction of chemical species, temperature, density etc. The R.H.S. of Eq. (1) describes the inflow and outflow events in a partially stirred reactor, with the characteristic residence time τ. S_l denotes the chemical source term for the species. In the present paper, we employ the IEM (Interaction by exchange with the mean) mixing model. The coefficients of Eq. (1) are:

$$A_l = -B(\psi_l - \langle\phi_l\rangle), \quad B = \frac{C_\phi}{2\tau_m} \tag{3}$$

where τ_m is the characteristic mixing time and $\langle\phi_l\rangle$ is the Favre average mean given by

$$\langle\phi_l\rangle = \frac{\int_{-\infty}^{\infty} \psi_l \mathcal{F}(\psi,t)d\psi}{\int_{-\infty}^{\infty} \mathcal{F}(\psi,t)d\psi}. \tag{4}$$

The initial condition for the MDF is a double delta distribution:

$$\mathcal{F}_0(\psi) = \left[\frac{\delta_{\psi^1}(\psi) + \delta_{\psi^2}(\psi)}{2}\right]. \tag{5}$$

In this investigation, we implement two different conditions for inflow:

1. Delta distribution:
$$\mathcal{F}_{in}(\psi) = \delta_{\psi_{in}}(\psi). \tag{6}$$
2. Uniform distribution:
$$\mathcal{F}_{in}(\psi) = \begin{cases} 1 & \text{for}, 0.0 < \psi < 1.0 \\ 0 & \text{elsewhere.} \end{cases} \tag{7}$$

In order to carry out a systematic numerical investigation, four different Cauchy problems of ascending complexity are addressed in this section. These Cauchy problems are obtained from Eq. (1), and describe the following events: inflow-outflow, inflow-outflow + reaction, inflow-outflow + mixing and inflow-outflow + reaction + mixing. The analytical solutions for the MDF, in case of inflow-outflow+mixing and inflow-outflow+mixing+reaction, as mentioned by Kraft [10], are valid only in a particular case with inflow, $\mathcal{F}_{in} = 0$. As an extension of the work carried out by Kraft [10], more general analytical solutions of the MDF and its first four moments for the different Cauchy problems are presented next.

2.1 Inflow-Outflow

The inflow-outflow term on the R.H.S. of Eq. (1) makes the equation inhomogeneous. We first investigate the inflow-outflow events without considering mixing and reactions. Thus, Eq. (1) simplifies to,

$$\frac{\partial}{\partial t}\mathcal{F}(\psi,t) = \frac{1}{\tau}(\mathcal{F}_{in}(\psi) - \mathcal{F}(\psi,t)). \tag{8}$$

with initial condition $\mathcal{F}(\psi,0)=\mathcal{F}_0(\psi)$.

The solution of the MDF is given by:

$$\mathcal{F}(\psi,t)=\mathcal{F}_{in}(\psi)\left(1-e^{\left(\frac{-t}{\tau}\right)}\right)+\mathcal{F}_0(\psi)e^{\left(\frac{-t}{\tau}\right)} \tag{9}$$

Moments

$$m_j=\int_{-\infty}^{\infty}\psi^j\mathcal{F}(\psi,t)d\psi, \tag{10}$$

$$m_j^{in}=\int_{-\infty}^{\infty}\psi^j\mathcal{F}_{in}(\psi,t)d\psi, \qquad j=0,1,2,3,\ldots. \tag{11}$$

The analytical solution for the moments of the MDF is given by:

$$m_j(t)=m_j^{in}+e^{-t/\tau}(m_j(0)-m_j^{in}) \qquad j=0,1,2,3,\ldots. \tag{12}$$

2.2 Inflow-Outflow + Reaction

The inflow-outflow and reaction events can be described by:

$$\frac{\partial\mathcal{F}(\psi,t)}{\partial t}-\frac{\partial}{\partial\psi}(k\psi)\mathcal{F}(\psi,t)=\frac{\mathcal{F}_{in}(\psi)}{\tau}-\frac{\mathcal{F}(\psi,t)}{\tau}. \tag{13}$$

Employing the method of characteristics, two ODEs for $\psi(t)$ and $\mathcal{F}(\psi,t)$ are obtained.

$$\frac{d\psi}{dt}=-k\psi \tag{14}$$

$$\frac{d\mathcal{F}(\psi(t),t)}{dt}=\frac{\mathcal{F}_{in}(\psi(t))}{\tau}+\left(k-\frac{1}{\tau}\right)\mathcal{F}(\psi(t),t) \tag{15}$$

Solving Eq. (14), the inverse characteristic curve is

$$\psi^*=\psi e^{kt}. \tag{16}$$

Solving the ODE for $\mathcal{F}(\psi(t),t)$:

$$\mathcal{F}(\psi(t),t)e^{\left(\frac{1}{\tau}-k\right)t}=\int\left[\frac{\mathcal{F}_{in}(\psi(t))}{\tau}\right]e^{\left(\frac{1}{\tau}-k\right)t}dt+C_I$$

where C_I is a constant of integration. The solution for MDF is obtained by substituting the conditions for the inflow, $\mathcal{F}_{in}$

Inflow as delta distribution:

Substituting the condition for $\mathcal{F}_{in}$, as given in Eq. (6):

$$\mathcal{F}(\psi(t),t)e^{\left(\frac{1}{\tau}-k\right)t}=\int\left[\frac{\delta(\psi(t)-\psi_{in})}{\tau}\right]e^{\left(\frac{1}{\tau}-k\right)t}dt+\acute{C}_I(\psi^*). \tag{17}$$

From the Eq. (16),

$$t = (-1/k) \ln \left[\frac{\psi}{\psi^*} \right]. \tag{18}$$

Thus

$$\mathcal{F}(\psi, t) e^{\left(\frac{1}{\tau} - k\right)t} = \left(\frac{-1}{k\tau} \right) \int \frac{\delta(\psi - \psi_{in})}{{\psi^*}^{(1-1/k\tau)}} \psi^{(-1/k\tau)} d\psi + \acute{C}_I(\psi^*)$$

$$\mathcal{F}(\psi, t) e^{\left(\frac{1}{\tau} - k\right)t} = \begin{cases} \left(\frac{-1}{k\tau}\right) \frac{(\psi_{in})^{(-1/k\tau)}}{(\psi^*)^{1-1/k\tau}} + \acute{C}_I(\psi^*) & \psi \geq \psi_{in}, \\ \acute{C}_I(\psi^*) & \psi \leq \psi_{in} \end{cases}$$

which is equivalent to:

$$\mathcal{F}(\psi, t) = \begin{cases} C_I(\psi^*) e^{\left(k - \frac{1}{\tau}\right)t} & \psi \geq \psi_{in}, \\ \left(\frac{1}{k\tau}\right) \frac{(\psi_{in})^{(-1/k\tau)}}{(\psi)^{1-1/k\tau}} + C_I(\psi^*) e^{\left(k - \frac{1}{\tau}\right)t} & \psi \leq \psi_{in} \end{cases}$$

Substituting the initial condition

$$t = 0, \quad \psi = \psi^* \quad \text{and} \quad \mathcal{F}(\psi(0), 0) = \mathcal{F}_0(\psi^*)$$

$$\mathcal{F}_0(\psi^*) = \begin{cases} C_I(\psi^*) & \psi^* \geq \psi_{in}, \\ C_I(\psi^*) + \frac{{\psi_{in}}^{(-1/k\tau)}}{k\tau} {\psi^*}^{[(1/k\tau)-1]} & \psi^* \leq \psi_{in} \end{cases}$$

The value of the constant of integration, $C_I(\psi^*)$ is:

$$C_I(\psi e^{(kt)}) = \begin{cases} \mathcal{F}_0(\psi e^{(kt)}) & \psi \geq \psi_{in} e^{(-kt)} \\ \mathcal{F}_0(\psi e^{(kt)}) - \frac{{\psi_{in}}^{(-1/k\tau)}}{k\tau} \left(\psi^{[(1/k\tau)-1]} e^{\left(\frac{1}{\tau} - k\right)t} \right) & \psi \leq \psi_{in} e^{(-kt)} \end{cases} \tag{19}$$

Thus ψ will have three regimes: $\psi \geq \psi_{in}$, $\psi_{in} e^{(-kt)} \leq \psi \leq \psi_{in}$ and $\psi \leq \psi_{in} e^{(-kt)}$.
Corresponding MDF:

$$\mathcal{F}(\psi, t) = \begin{cases} \mathcal{F}_0(\psi e^{(kt)}) e^{\left(k - \frac{1}{\tau}\right)t} & \psi \geq \psi_{in}, \\ \mathcal{F}_0(\psi e^{(kt)}) e^{\left(k - \frac{1}{\tau}\right)t} + \frac{{\psi_{in}}^{(-1/k\tau)}}{k\tau} \psi^{[(1/k\tau)-1]} & \psi_{in} e^{(-kt)} \leq \psi \leq \psi_{in}, \\ \mathcal{F}_0(\psi e^{(kt)}) e^{\left(k - \frac{1}{\tau}\right)t} & \psi \leq \psi_{in} e^{(-kt)}. \end{cases} \tag{20}$$

Inflow as a uniform distribution:
Substituting the inflow condition: We get,

$$\mathcal{F}(\psi(t), t) e^{\left(\frac{1}{\tau} - k\right)t} = \int_0^t \frac{\mathcal{F}_{in}(\psi(t))}{\tau} e^{\left(\frac{1}{\tau} - k\right)t} dt$$

$$= \int_0^{\frac{1}{k} \ln \psi^*} \frac{\mathcal{F}_{in}(\psi(t))}{\tau} e^{\left(\frac{1}{\tau} - k\right)t} dt + \int_{\frac{1}{k} \ln \psi^*}^t \frac{\mathcal{F}_{in}(\psi(t))}{\tau} e^{\left(\frac{1}{\tau} - k\right)t} dt.$$

Now, $\mathcal{F}_{in}$ is equal to 1.0, for the condition: $0 < \psi < 1.0$, which is equivalent to: $\frac{1}{k}\ln(\psi^*) < t < \infty$.

$$\mathcal{F}(\psi(t),t) = \mathcal{F}_0(\psi^*)e^{\left(k-\frac{1}{\tau}\right)t} + \frac{1}{(1-k\tau)}\begin{cases} 1-e^{\left(k-\frac{1}{\tau}\right)t} & \psi^* < 1.0 \\ 1-\psi^{*\left(\frac{1}{k\tau}-1\right)}e^{\left(k-\frac{1}{\tau}\right)t} & \psi^* > 1.0 \end{cases} \tag{21}$$

Analytical solutions for the moments of the MDF are obtained as follows: The procedure to obtain the zeroth moment of the MDF is given below. The same procedure is followed to obtain first, second and third moments.

$$\begin{aligned} m_0 &= \int_{-\infty}^{\infty} \mathcal{F}(\psi,t)d\psi \qquad (22) \\ \frac{dm_0}{dt} &= \int_{-\infty}^{\infty}\left[\frac{\mathcal{F}_{in}(\psi)}{\tau} - \frac{\mathcal{F}(\psi,t)}{\tau} + k\psi\frac{\partial\mathcal{F}(\psi,t)}{\partial\psi} + k\mathcal{F}(\psi,t)\right]d\psi. \\ m_0(t) &= m_0^{in} + (m_0(0) - m_0^{in})e^{\left(\frac{-t}{\tau}\right)}. \end{aligned}$$

In general, the analytical solution for the moments of the MDF is given as:

$$m_j(t) = \frac{m_j^{in}}{(1+jk\tau)} + \left[m_j(0) - \frac{m_j^{in}}{(1+jk\tau)}\right]e^{-\left(jk+\frac{1}{\tau}\right)t} \qquad j = 0,1,2,3,\ldots \tag{23}$$

2.3 Inflow-Outflow + Mixing

The inflow-outflow and mixing events are described by:

$$\frac{\partial\mathcal{F}(\psi,t)}{\partial t} - \frac{\partial}{\partial\psi}\left(B(\psi - \langle\phi\rangle)\right)\mathcal{F}(\psi,t) = \frac{\mathcal{F}_{in}(\psi)}{\tau} - \frac{\mathcal{F}(\psi,t)}{\tau} \tag{24}$$

with initial condition $\mathcal{F}(\psi,0) = \mathcal{F}_0(\psi)$. In this (inflow-outflow+reaction) and the next case (inflow-outflow+mixing+reaction), solving the characteristic curve does not yield an explicit relation between t and ψ. Thus the transformation of variable from dt to $d\psi$ is not possible, as that in Eq. (18) and hence the analytical solution for the MDF cannot be obtained by our method. However, the analytical solutions for the first four moments of the MDF are obtained, as explained previously. The

analytical solutions for the moments of MDF are as follows:

$$m_0(t) = m_0^{in} + (m_0(0) - m_0^{in})e^{-t/\tau} \tag{25}$$

$$m_1(t) = m_1^{in} + (m_1(0) - m_1^{in})e^{-t/\tau} \tag{26}$$

$$\begin{aligned} m_2(t) = {} & \frac{m_2^{in}}{2B\tau+1}\left(1 - e^{-(2B+\frac{1}{\tau})}\right) + e^{-(2B+\frac{1}{\tau})t}\Bigg(m_2(0) + \frac{2B}{m_0(0)}\times \\ & \Big[\frac{(m_1(0)-m_1^{in})^2}{(2B-\frac{1}{\tau})}(e^{(2B-\frac{1}{\tau})t}-1) + \frac{m_1^{in}(m_1(0)-m_1^{in})}{B}(e^{2Bt}-1) \\ & + \frac{(m_1^{in})^2}{2B+\frac{1}{\tau}}(e^{2B+\frac{1}{\tau}}-1)\Big]\Bigg) \end{aligned} \tag{27}$$

$$m_3(t) = \frac{m_3^{in}(1 - e^{-(3B+\frac{1}{\tau})})}{(3B\tau+1)} + (m_3(0) + 3BL)e^{-(3B+\frac{1}{\tau})t}$$

where,

$$\begin{aligned} L = m_1^{in}\Bigg[& \Bigg(\frac{(m_2(0) - 2m_1(0)m_1^{in} + 2\,(m_1^{in})^2)}{B} - \frac{m_2^{in} + 2B\tau(m_1^{in})^2}{B(2B\tau+1)} \\ & - \frac{(2\tau(m_1^{in} - m_1(0))^2)}{(2B\tau-1)}\Bigg)\big[e^{Bt}-1\big] + \frac{(2m_1(0)m_1^{in} - 2m_1^{in^2})}{3B}\big[e^{(3Bt)}-1\big] \\ & + \frac{2B\tau(m_1^{in} - m_1(0))^2}{(2B\tau-1)(3B-\frac{1}{\tau})}\big[e^{(3B-\frac{1}{\tau})t}-1\big] + \frac{(m_2^{in} + 2B\tau(m_1^{in})^2)}{(2B\tau+1)(3B+\frac{1}{\tau})}\big[e^{(3B+\frac{1}{\tau})t}-1\big]\Bigg] \\ & + (m_1(0) - m_1^{in})\Bigg[\Bigg(\frac{(m_2(0) - 2m_1(0)m_1^{in} + 2\,(m_1^{in})^2)}{(B-\frac{1}{\tau})} - \frac{m_2^{in} + 2B\tau(m_1^{in})^2}{(B-\frac{1}{\tau})(2B\tau+1)} \\ & - \frac{(2B\tau(m_1^{in} - m_1(0))^2)}{(B-\frac{1}{\tau})(2B\tau-1)}\Bigg)\big[e^{(B-\frac{1}{\tau})t}-1\big] + \frac{(2m_1(0)m_1^{in} - 2m_1^{in^2})}{(3B-\frac{1}{\tau})}\big[e^{(3B-\frac{1}{\tau})t}-1\big] \\ & + \frac{2B\tau(m_1^{in} - m_1(0))^2}{(2B\tau-1)(3B-\frac{2}{\tau})}\big[e^{(3B-\frac{2}{\tau})t}-1\big] + \frac{(m_2^{in} + 2B\tau(m_1^{in})^2)}{(2B\tau+1)(3B)}\big[e^{(3B)t}-1\big]\Bigg]. \end{aligned}$$

2.4 Inflow-Outflow + Mixing + Reaction

Finally we present the most complicated Cauchy problem. The inflow-outflow, mixing and reaction events are described by:

$$\frac{\partial \mathcal{F}(\psi,t)}{\partial t} - \frac{\partial}{\partial \psi}\big(B(\psi - \langle\phi\rangle) + k\psi\big)\mathcal{F}(\psi,t) = \frac{\mathcal{F}_{in}(\psi)}{\tau} - \frac{\mathcal{F}(\psi,t)}{\tau} \tag{27}$$

with initial condition $\mathcal{F}(\psi,0)=\mathcal{F}_0(\psi)$. The analytical solution for the moments of MDF are as given below:

$$
\begin{aligned}
m_0(t) &= m_0^{in} + (m_0(0) - m_0^{in})e^{-t/\tau} \\
m_1(t) &= \frac{m_1^{in}(1-e^{-\left(k+\frac{1}{\tau}\right)t})}{(k\tau+1)} + m_1(0)e^{-\left(k+\frac{1}{\tau}\right)t} \\
m_2(t) &= \frac{m_2^{in}(1-e^{-(2B+2k+\frac{1}{\tau})t})}{(2B\tau+2k\tau+1)} + (m_2(0)+2BG)e^{-(2B+2k+\frac{1}{\tau})t} \\
m_3(t) &= \frac{m_3^{in}(1-e^{-(3B+3k+\frac{1}{\tau})t})}{(3B\tau+3k\tau+1)} + (m_3(0)+3BT)e^{-(3B+3k+\frac{1}{\tau})t}
\end{aligned}
$$

where,

$$
H = -\frac{(m_1(0))^2}{(2B-\frac{1}{\tau})} + \frac{2m_1(0)m_1^{in}}{\tau(2B-\frac{1}{\tau})(2B+k)} - \frac{(m_1^{in})^2(2k^2+\frac{4k}{\tau}+\frac{2}{\tau^2})}{(1+k\tau)^2(2B+k)(2B-\frac{1}{\tau})(2B+2k+\frac{1}{\tau})}
$$

$$
\begin{aligned}
G = &\left(m_1(0) - \frac{m_1^{in}}{(1+k\tau)}\right)^2 \frac{e^{(2B-\frac{1}{\tau})t}}{(2B-\frac{1}{\tau})} + \left(\frac{(m_1^{in})^2}{(2B+2k+\frac{1}{\tau})(1+k\tau)^2}\right) e^{\left(2B+2k+\frac{1}{\tau}\right)t} \\
&+ \left[\frac{2m_1(0)m_1^{in}}{1+k\tau} - \frac{2\,(m_1^{in})^2}{(1+k\tau)^2}\right] \frac{e^{(2B+k)t}}{(2B+k)} + H
\end{aligned}
$$

$$
\begin{aligned}
T = &\left(m_1(0) - \frac{m_1^{in}}{(1+k\tau)}\right) \left[\frac{(m_2(0)+2BH-\frac{m_2^{in}}{(2B\tau+2k\tau+1)})}{(B-\frac{1}{\tau})}\left[e^{(B-\frac{1}{\tau})t}-1\right]\right. \\
&+ \left(\frac{2B\,(m_1^{in})^2}{(1+k\tau)^2} + \frac{m_2^{in}}{\tau}\right) \frac{\left[e^{(3B+2k)t}-1\right]}{(2B+2k+\frac{1}{\tau})(3B+2k)} \\
&+ \frac{2B}{(2B-\frac{1}{\tau})}\left(m_1(0) - \frac{m_1^{in}}{(1+k\tau)}\right) \frac{\left[e^{(3B-\frac{2}{\tau})t}-1\right]}{(3B-\frac{2}{\tau})} \\
&\left.+ \frac{4B}{(2B+k)}\left(\frac{m_1(0)m_1^{in}}{(1+k\tau)} - \frac{(m_1^{in})^2}{(1+k\tau)^2}\right) \frac{\left[e^{(3B+k-\frac{1}{\tau})t}-1\right]}{(3B+k-\frac{1}{\tau})}\right] \\
&+ \left(\frac{m_1^{in}}{1+k\tau}\right) \left[\frac{(m_2(0)+2BH-\frac{m_2^{in}}{(2B\tau+2k\tau+1)})}{(B+k)}\left[e^{(B+k)t}-1\right]\right. \\
&+ \left(\frac{2B\,(m_1^{in})^2}{(1+k\tau)^2} + \frac{m_2^{in}}{\tau}\right) \frac{\left[e^{(3B+3k+\frac{1}{\tau})t}-1\right]}{(2B+2k+\frac{1}{\tau})(3B+3k+\frac{1}{\tau})} \\
&+ \frac{2B}{(2B-\frac{1}{\tau})}\left(m_1(0) - \frac{m_1^{in}}{(1+k\tau)}\right) \frac{\left[e^{(3B+k-\frac{1}{\tau})t}-1\right]}{(3B+k-\frac{1}{\tau})} \\
&\left.+ \frac{4B}{(2B+k)}\left(\frac{m_1(0)m_1^{in}}{(1+k\tau)} - \frac{(m_1^{in})^2}{(1+k\tau)^2}\right) \frac{\left[e^{(3B+2k)t}-1\right]}{(3B+2k)}\right]
\end{aligned}
$$

The analytical solutions developed here are exploited for a detailed numerical investigation of the Monte Carlo particle method. The following section deals with the description of a Monte Carlo particle algorithm implemented with a first order time splitting technique.

3 Numerical solution

A Monte Carlo particle method with time splitting procedure is adopted to obtain the first four moments of the MDF numerically. The numerical method is explained in detail in this section. Monte Carlo particle algorithms involve the approximation of the initial density function by a notional particle ensemble. These particles are then moved according to the evolution equation of the corresponding density function [17, 15].

In the present work, the system of stochastic particles is introduced as

$$\psi^{(1)}(t), \psi^{(2)}(t), \ldots, \psi^{(N)}(t), \quad t > 0.$$

The MDF ($\mathcal{F}$) is approximated by,

$$\mathcal{F} \approx \mathcal{F}^N = \frac{1}{N} \sum_{n=1}^{N} \delta_{\psi^{(n)}}$$

A time splitting algorithm is implemented in which the inflow-outflow, mixing and reaction events are treated sequentially, in a given time step Δt.

Monte Carlo particle method with first order time splitting algorithm is given as follows:

1. Determine the state of the system of particles (3) at time 0, according to initial function $\mathcal{F}_0$
2. Given the state of the system at time $t \longrightarrow t + \Delta t$, perform *inflow-outflow* step.
3. Given the system at time t, each particle is moved according to the *reaction* step.
4. Given the system at time t, each particle in the ensemble is moved according to the *mixing* step.
5. If time exceeds termination time then STOP! Else, go to Step 2.

The individual mixing, reaction, and inflow-outflow events and their implementation in the particle algorithm are discussed next.

3.1 Mixing

The IEM model (also known as linear mean square estimation (LMSE) model) is a deterministic model that does not introduce any fluctuations. Simplicity and less computational effort are the salient features of this model. The model works on the principle that the scalar value of each particle approaches the mean scalar value of all the particles with a characteristic time τ_m. The molecular mixing term in Eq. (1) is closed by the IEM model:

$$\frac{d\psi^{(i)}(t)}{dt} = -B(\psi^{(i)}(t) - \langle\phi\rangle) \tag{24}$$

where i is the index for the particle number and $\langle\phi\rangle$ is the empirical mean calculated at time t_0.

$$\frac{d\psi^{(i)}(t)}{dt} = -B\left[\psi^{(i)}(t) - \frac{1}{N}\sum_{j=1}^{N}\psi^{(j)}(t)\right].$$

For the IEM model,

$$\frac{d}{dt}\frac{1}{N}\sum_{i=1}^{N}\psi^{(i)}(t) = 0.$$

The solution is given as

$$\psi^{(i)} = \psi^{(i)}(t_0)e^{-B\Delta t} + \left[1 - e^{-B\Delta t}\right]\frac{1}{N}\sum_{j=1}^{N}\psi^{(j)}(t_0) \tag{22}$$

where, $\Delta t = t - t_0$. At each time step, the particle ensemble is updated as per the mixing model.

3.2 Reaction

The reaction step is given by

$$\frac{d}{dt}\psi_l^{(i)}(t) = S_l(\psi^{(i)}(t)). \tag{22}$$

For a linear reaction $A \longrightarrow B$,

$$\frac{d}{dt}\psi^{(i)}(t) = -k(\psi^{(i)}(t)). \tag{22}$$

The rate equation can be solved analytically to obtain:

$$\psi^{(i)}(t) = \left(\psi^{(i)}(t_0)\right)e^{-k\Delta t}, \quad \Delta t = t - t_0.$$

3.3 Inflow-Outflow

Correa and Braaten [6] stated the number of inflow particles N_{in}, within a time step Δt as:

$$N_{in} \approx \frac{\dot{m} \times \Delta t}{m_p} \tag{22}$$

where m_p is the mass of a particle and $\dot{m}$ is the mass flow rate. Chen [5], incorporated the total reactor mass (M), and the residence time (τ):

$$N_{in} \approx \frac{\Delta t}{(M/N\dot{m})} \approx \frac{\Delta t \times N}{\tau} \tag{22}$$

The underlying assumption in the inflow-outflow models is that the particles which are selected according to uniform distribution, flow out at the same rate. Three different inflow-outflow algorithms are explained.

3.3.1 Algorithm 1

This section contains a stochastic algorithm for inflow-outflow event modelled as a poisson process [7]. The particle system is as given in Eq. (3). The dynamics of the particle system can be described by a sequence of jump processes

$$U^N(t), \quad t \geq 0, \quad N = 1, 2, 3, \ldots$$

taking values in the space of discrete measures

$$\mathcal{S}^N = \{p = \frac{1}{N}\sum_{i=1}^{N} \delta_{\psi^{(i)}}, \quad \psi^i > 0, \quad N = 1, 2, \ldots\}$$

The generator of a stochastic process relates time evolution of the PDF of a stochastic process with the time evolution of the process itself. The *infinitesimal stochastic generator* is given by,

$$\mathcal{A}^N \Phi(p) = \sum_{i=1}^{N} K(\psi^{(i)}) \int_{\mathbb{R}} [\Phi(J(p, \gamma, i)) - \Phi(p)] \mathcal{F}_{in}(\gamma) d\gamma \tag{20}$$

where,

$$\Phi(p) = \int \varphi(\psi) p(., d\psi)$$

and φ is any test function.

Thus the rate is

$$\sum_{i=1}^{N} K(\psi^{(i)}) = \sum_{i=1}^{N} \frac{1}{\tau} = \frac{N}{\tau}$$

and

$$J(p, \gamma, i) = p + \frac{\delta_\gamma}{N} - \frac{\delta_{\psi(i)}}{N}.$$

Between each finite time step Δt, the sequence of stochastic jump processes (algorithm 1) is implemented in the time splitting algorithm as follows:

1. Given the state at time t, $U^N(t) = p \in \mathcal{S}^N$
2. Wait an exponentially distributed time step $\hat{\tau}$ with parameter

$$\pi(p) = \frac{N}{\tau}$$

   where

$$\text{Prob}\{\hat{\tau} \geq t\} = e^{-\pi(p)t}.$$

3. Update time $t \longrightarrow t + \hat{\tau}$. If $(t > t + \Delta t)$ then STOP; Else go to Step 4
4. Choose a particle index i according to the mass density

$$g_i = \frac{1}{N} \qquad i \in \{1, 2, \ldots, N\}.$$

5. Generate a $\mathcal{F}_{in}$ deviate γ and replace particle at position i.
6. go to Step 2.

3.3.2 Algorithm 2

From the Section 3.3.1, the deterministic waiting time is given as

$$dt_\omega = \pi^{-1}(p) = \frac{\tau}{N} \tag{16}$$

With a specified time step Δt, the number of particles to be replaced (N_{in}) in this time step is given by

$$N_{in} = \frac{N\Delta t}{\tau} \tag{16}$$

according to

$$\Delta t = N_{in} dt_\omega = N_{in} \frac{\tau}{N}. \tag{16}$$

Equation (3.3.2) is equivalent to Eq. (3.3), implemented to calculate the number of particles to be replaced (N_{in}) in a single time step (Δt). Thus *algorithm 2 can be explained by considering a deterministic waiting time parameter of a corresponding stochastic process.*

3.3.3 Algorithm 3

In this section, algorithm 3 is derived on the basis of the analytical solution of the MDF describing the inflow-outflow event. The analytical solution of the split Cauchy problem, as stated in Eq. (24), is given by,

$$\mathcal{F}(\psi,t) = (1-A)\mathcal{F}_{in}(\psi) + A\mathcal{F}_0(\psi) \tag{16}$$

where, $A = e^{-\frac{(t-t_0)}{\tau}}$. Representing the analytical solution as a measure:

$$\int \mathcal{F}(\psi,t)\varphi(\psi)d\psi = \int (1-A)\mathcal{F}_{in}(\psi)\varphi(\psi)d\psi + \int A\mathcal{F}_0(\psi)\varphi(\psi)d\psi$$

An approximation to this measure valued solution can be obtained by approximating the initial and the inflow distributions independently. Approximating the solution with an equi-weighted particle ensemble for $\mathcal{F}_{in}$ and $\mathcal{F}_0$ distributions, N_{in} particles are used to form the inlet distribution and N_0 particles for the initial distribution.

$$\mathcal{F}_{in}(\psi) \approx \sum_{n=1}^{N_{in}} \frac{1}{N_{in}} \delta_{\psi_{in}^{(n)}}$$

$$\mathcal{F}_0(\psi) \approx \sum_{n=1}^{N_0} \frac{1}{N_0} \delta_{\psi_0^{(n)}}.$$

Therefore,

$$\mathcal{F}(\psi,t) \approx (1-A)\frac{1}{N_{in}} \sum_{n=1}^{N_{in}} \delta_{\psi_{in}^{(n)}} + \frac{A}{N_0} \sum_{n=1}^{N_0} \delta_{\psi_0^{(n)}}.$$

Thus, the approximation includes $N = N_{in} + N_0$ particles. An equi-weighted particle ensemble is constructed with N particles. For the single approximations of $\mathcal{F}_0$ and $\mathcal{F}_{in}$, the number of particles are obtained as,

$$N_0(t) = N \times A(t) \tag{13}$$
$$N_{in}(t) = N \times (1 - A(t)) \tag{14}$$

$$\mathcal{F}(\psi,t) \approx \frac{1}{N} \sum_{n=1}^{N_0} \delta_{\psi_0^{(n)}} + \frac{1}{N} \sum_{n=1}^{N_{in}} \delta_{\psi_{in}^{(n)}}$$

Therefore,

$$\int \mathcal{F}(\psi,t)\varphi(\psi)d\psi \approx \frac{1}{N}\sum_{n=1}^{N_0} \varphi(\psi_0^{(n)}) + \frac{1}{N}\sum_{n=1}^{N_{in}} \varphi(\psi_{in}^{(n)})$$

Time marching: The particle representation of the analytical solution is used to construct a numerical scheme. A representative time step $t \longrightarrow t + \Delta t$ is considered for demonstration: At time t the total number of particles is N. With the time step Δt, the particles at time t decay according to the relation

$$N_0(t + \Delta t) = A(t + \Delta t) \times N \tag{12}$$

Therefore, the number of inflow particles N_{in} is given by

$$N_{in}(t + \Delta t) = N - N_0(t + \Delta t) \tag{12}$$

In every time step, $N_{in} = N\left[1 - e^{\frac{-\Delta t}{\tau}}\right]$ particles are replaced from the particle ensemble of size N, according to uniform distribution.

At this point we discuss three different ways in which the algorithm 3 can be implemented in the Monte Carlo particle algorithm with time splitting.

3.3.4 Implementation of algorithm 3 in the time splitting algorithm

Given a time step Δt, algorithm 3 gives the exact number of inflow particles N_{in}. The three different ways of implementing the inflow-outflow step are described below;

1. In a time step Δt, N_{in} *distinct* particles are chosen from the ensemble according to uniform distribution and replaced by the inflow particles.

2. n particles are chosen (allowing non-distinct particles to be chosen) in a time step Δt according to uniform distribution, and replaced with the inflow particles.

   n is given by:

   $$n = \frac{-\frac{\Delta t}{\tau}}{\ln\left[1 - \frac{1}{N}\right]} \tag{12}$$

   Proof: The size of the particle ensemble is N. n indices are chosen according to uniform distribution $U[1, N]$. Let X_i where $i = 1, 2, \ldots, n$ be the random variable that denotes the particle index. If $Y_{n,N}$ is the random variable which represents the number of distinct X_i values, then we can choose the expectation of Y to be equal to the required number of inflow particles, N_{in}, as given by algorithm 3. The expectation is obtained as follows:

   The probability of j distinct indices to occur in n is;

   $$p(n, j) = P(Y_N = j) = p(n - 1, j) \times \frac{j}{N} + p(n - 1, j - 1) \times \frac{N - (j - 1)}{N} \tag{12}$$

   Now, expectation is given by

   $$E(Y_{N,n} = j) = \sum_{j=1}^{n} j \times p(n, j)$$

$$
\begin{aligned}
&= \sum_{j=1}^{n} jp(n-1,j)\frac{j}{N} + \sum_{j=1}^{n} jp(n-1,j-1)\frac{(N-(j-1))}{N} \\
&= \sum_{j=1}^{n} jp(n-1,j)\frac{j}{N} + \sum_{\acute{j}=2}^{n} jp(n-1,\acute{j}-1)\frac{(N-(\acute{j}-1))}{N} \\
&= \sum_{j=1}^{n-1} jp(n-1,j)\frac{j}{N} + \sum_{j=1}^{n-1} (j+1)p(n-1,j)\frac{(N-j)}{N} \\
&= \sum_{j=1}^{n-1} \left[\frac{j^2}{N} + \frac{(j+1)(N-j)}{N}\right] p(n-1,j) \\
&= \sum_{j=1}^{n-1} p(n-1,j) + \sum_{j=1}^{n-1} \left(\frac{N-1}{N}\right) jp(n-1,j) \\
&= 1 + \left(\frac{N-1}{N}\right) \sum_{j=1}^{n-1} jp(n-1,j)
\end{aligned}
$$

Therefore,

$$E_n = 1 + \frac{(N-1)}{N} E_{n-1}$$

The solution is of the form

$$E_n = N - cx^n$$

Thus,

$$N - cx^n = 1 + \frac{(N-1)}{N}(N - cx^{n-1})$$

$x = \frac{N-1}{N}$ or 0. Using, $n = 0, E_0 = 0$. Therefore $N = c$.
Thus,

$$E_n = N\left[1 - \left(\frac{N-1}{N}\right)^n\right] \tag{3}$$

Substituting the expectation as N_{in}

$$N_{in} = N\left[1 - \left(\frac{N-1}{N}\right)^n\right] \tag{3}$$

Therefore,

$$n = \frac{-\frac{\Delta t}{\tau}}{\ln\left[1 - \frac{1}{N}\right]} \tag{3}$$

As $N \longrightarrow \infty$, neglecting the higher order terms the equation becomes

$$n = N\frac{\Delta t}{\tau} \tag{3}$$

The expression for n resembles the number of inflow particles as calculated by algorithm 2, in Eq. (3.3.2)

3. Consider a representative time step $t \longrightarrow t + \Delta t$. At time t, the ensemble consists of N_{in} - $\mathcal{F}_{in}$ distributed particles and N_0 - $\mathcal{F}_0$ distributed particles. With a time step Δt, the particle ensemble N representing $\mathcal{F}^N$ is down-sampled to size $N - N_{in}$, by choosing equivalent number of $\mathcal{F}_0$ and $\mathcal{F}_{in}$ distributed particles from the ensemble at time t, according to uniform distribution. N_{in} particles are added, thus retaining the size of the ensemble to N.

The three methods mentioned above are compared in terms of the CPU time consumed by each. At a value of $\frac{\Delta t}{\tau} < 1$, very few particles are exchanged in a time step. Hence, the CPU times consumed by methods 1 and 2 are same, whereas that consumed by method 3 is more by a factor of two. In the condition $\frac{\Delta t}{\tau} > 1$, methods 2 and 3 are faster than the method 1 by a factor of three. In this paper, method 1 is implemented.

3.3.5 Comparison of algorithm 2 with algorithm 3

In the case of algorithm 3, the number of particles exchanged (N_{in}), in a single time step Δt, is given by:

$$N_{in} = N - Ne^{(-\frac{\Delta t}{\tau})} \tag{3}$$

Expanding the exponential term using Taylor series expansion:

$$\begin{aligned} N_{in} &= N - \left\{ N - N\left(\frac{\Delta t}{\tau}\right) + N \times \mathcal{O}\left[\left(\frac{\Delta t}{\tau}\right)^2\right] \right\} \\ &= N\left(\frac{\Delta t}{\tau}\right) + \mathcal{O}\left[\left(\frac{\Delta t}{\tau}\right)^2\right] \end{aligned} \tag{3}$$

The first term on the right hand side of Equation (3) represents the number of particles exchanged in the case of algorithm 2. For the ratio $(\frac{\Delta t}{\tau}) << 1$, the higher order terms in the above equation become less significant; thus, the algorithm 2 is a special case of algorithm 3. The algorithm 2 fails for the condition $\Delta t > \tau$, as the number of particles to be replaced in a time step is greater than the number of particles in the ensemble.

The following section includes the numerical experiments carried out to study the convergence of the Monte Carlo particle method.

4 Convergence studies

For the Monte Carlo particle algorithm employed, there are three numerical parameters, the number of particles N, the number of independent simulation trials L and the splitting time step Δt that are the main sources of numerical error. In this section we investigate the convergence of the Monte Carlo particle method with respect to these numerical parameters. First, we introduce some definitions and notations used in the numerical procedures.

The estimation of an *interval*, which will include the parameter being estimated, with known degree of uncertainty is advantageous as compared to point estimation [1, 12]. The confidence intervals for the expectation of a random variable are determined and statistical and systematic errors are evaluated as follows:

Consider a functional, F, which represents, say the scalar mass fraction,

$$F = \int \varphi(\psi)\mathcal{F}(\psi;t)d\psi$$

where φ is a test function. The functional is approximated (as$N \longrightarrow \infty$) by the random variable,

$$\xi^N(t) = \int \varphi(\psi)\frac{1}{N}\sum_{i=1}^{N}\delta_{\psi^{(i)}}(d\psi) = \frac{1}{N}\sum_{i=1}^{N}\varphi(\psi^{(i)}).$$

The expectation and the random fluctuations of the estimator are estimated by generating L independent particle ensembles. The corresponding values of the random variable are denoted as $\xi^{N,1}(t),\ldots,\xi^{N,L}(t)$. The empirical mean value is given by:

$$\eta_1^{N,L}(t) = \frac{1}{L}\sum_{n=1}^{L}\xi^{N,n}(t).$$

The variance of the random variable is estimated by the empirical variance

$$\eta_2^{N,L}(t) = \frac{1}{L}\sum_{n=1}^{L}\left[\xi^{N,n}(t)\right]^2 - \left[\eta_1^{N,L}(t)\right]^2$$

The empirical mean is used to approximate the macroscopic quantity (mass fraction). The confidence interval for the expectation of the random variable is given by

$$I_p = \left[\eta_1^{N,L}(t) - a_p\sqrt{\frac{\eta_2^{N,L}(t)}{L}}, \eta_1^{N,L}(t) + a_p\sqrt{\frac{\eta_2^{N,L}(t)}{L}}\right]$$

The approximation as given in Eq. (4) leads to an error

$$\epsilon^{(N,L)}(t) = |{\eta_1}^{(N,L)}(t) - F(t)|$$

with two components, statistical error and systematic error. Throughout the paper, confidence level $p = 0.999$ and $a_p = 3.29$ is used. With the evolution in time t such that $t_i = i\Delta t$, the measure for the statistical error is :

$$c_{stats} = \max \left\{ a_p \sqrt{\frac{\eta_2^{N,L}(t_i)}{L}} \right\}. \qquad (-1)$$

Thus, statistical error scales as $N^{-1/2}$ and $L^{-1/2}$, in agreement with Xu and Pope [19]. The maximum value of the absolute difference between empirical moment and analytical moment is c_{tot} which is used as a measure for systematic error. In the following sections, we investigate separately the influence of the number of particles and the size of the time splitting step on the error.

4.1 Analysis of error with respect to time splitting

To study the effect of time splitting on the error, we split the analytical solutions for the moments of the MDF for the three events (inflow-outflow, reaction and mixing). Thus the error is independent of N. We compare the moments obtained from the split analytical solution with those from the non-split analytical solutions. For example, with a representative time step $\Delta t = t - t_0$, the second moment is given by:

Inflow-outflow

$$m_2(t) = m_2^{in} + (m_2(t_0) - m_2^{in})e^{-(\frac{\Delta t}{\tau})} \qquad (-1)$$

Reaction

$$m_2(t) = m_2(t_0)e^{-2(\frac{\Delta t}{\tau_r})} \qquad (-1)$$

Mixing

$$m_2(t) = m_2(t_0)e^{-2(\frac{C_\phi}{2})(\frac{\Delta t}{\tau_m})} + m_1(t_0)^2 \left(1 - e^{-2(\frac{C_\phi}{2})(\frac{\Delta t}{\tau_m})}\right) \qquad (-1)$$

The values for the various numerical parameters that are used in the simulations are as follows: The mixing model constant $C_\phi = 2$ [17]. The inflow condition, as given in Eq. (6), is set at $\psi_{in} = 0.9$. The strongest interactions between fluid mechanics and chemical kinetics are expected to occur when the characteristic times for the three events are of the same order of magnitude. Two distinct Damkohler numbers can be defined $Da_{res} = \frac{\tau}{\tau_r}$ and $Da_{mix} = \frac{\tau_m}{\tau_r}$. We choose the values of the characteristic times such that the two Damkohler numbers approach unity. The residence time is $\tau = 3.0s$, whereas the characteristic time for mixing is $\tau_m = 2.0s$, and the rate of the reaction is $k = 1s^{-1}$. For a linear reaction $A \longrightarrow B$, the reaction characteristic time $\tau_r = \frac{1}{k}$.

We define a dimensionless time step Δt^*, where

$$\Delta t^*_{event} = \frac{\text{time step}}{\text{characteristic time of an event}}$$

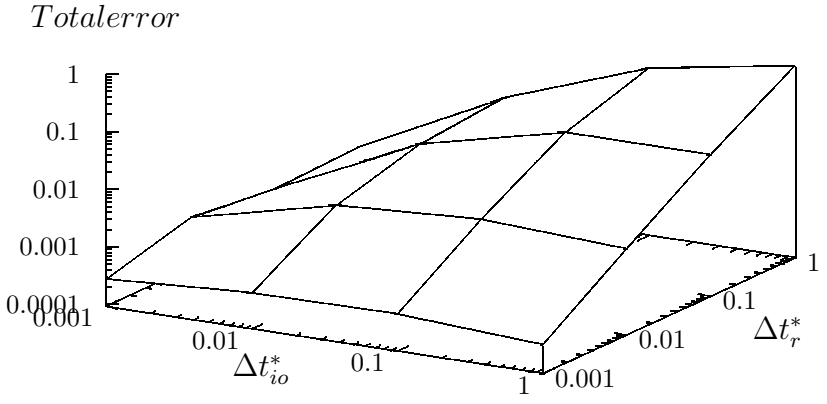

Figure 1: *Total error for moment 2, with respect to the dimensionless time steps for reaction and inflow-outflow events (inflow: delta distribution).*

Considering the case for inflow-outflow + reaction, **Figure** 1 depicts the error with respect to the dimensionless time steps for inflow-outflow and reaction events. With decrease in the dimensionless splitting time step, the error decreases. To study the order of convergence we consider the case, inflow-outflow+mixing+reaction. Δt^* is set according to the relation,

$$\Delta t^* = \frac{\Delta t}{\min(\tau, \tau_r, \tau_m)}.$$

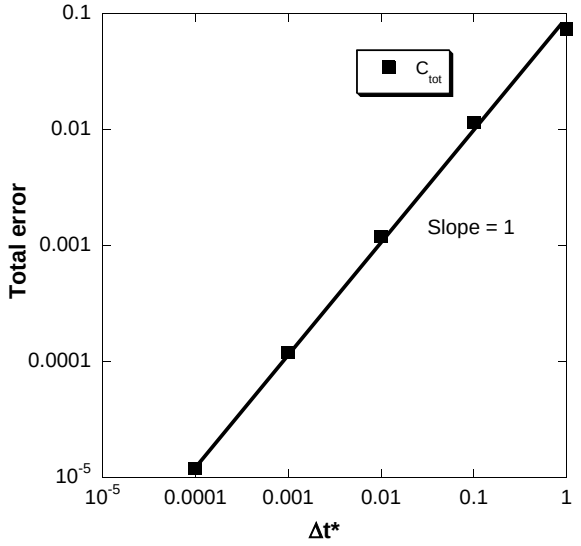

Figure 2: *Order of convergence with respect to Δt^*, for moment 2 (inflow as delta distribution)*

Figure 2 shows the error convergence with respect to the dimensionless time step (Δt^*). The *error scales as* Δt^*.

Having investigated the influence of the non-dimensional time step on the error, the effect of N on the error is studied by employing the Monte Carlo particle method with time splitting algorithm.

4.2 Analysis of error with respect to the number of particles

We implement the particle algorithm with time splitting. Statistical and systematic errors are calculated, and the order of convergence with respect to number of particles, N, is investigated in this section.

First we illustrate the comparison of the evolution of moments obtained numerically and analytically for a Cauchy problem describing inflow-outflow+mixing+reaction events. **Figure** 3(a) and **Figure** 3(b) depict the evolution of the first, second and third moments for the two different inflow conditions. For the values of N and Δt chosen, the numerical and analytical solutions for the moments show good agreement for both the inflow cases. To study the convergence with respect to N we consider two Cauchy problems; one describing the inflow-outflow event and the other for inflow+reaction+mixing events.

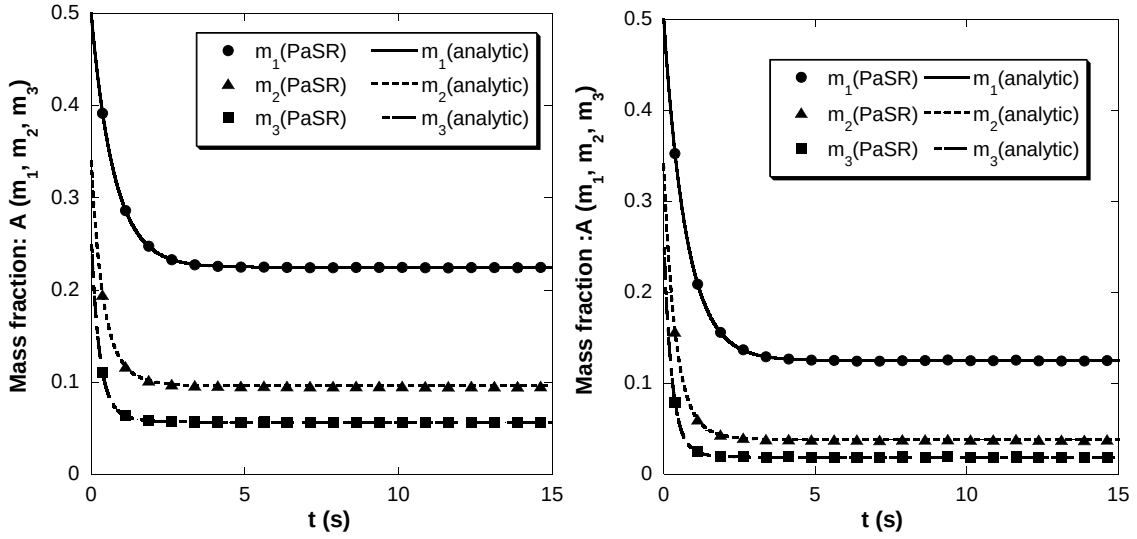

(a) Inflow as delta distribution

(b) Inflow as a uniform distribution

Figure 3: *Evolution of moments* ($N = 10^4, \Delta t = 0.001, k = 1s^{-1}, \tau = 3.0s, \tau_m = 2.0s$)

4.2.1 Inflow-Outflow

L independent runs (trials) of the particle ensemble are carried out to construct confidence bands with width c_{stats}. The product $L \times N = 200000$ is kept constant, in order to maintain the confidence bands roughly the same width for different calculations. The measured quantities (empirical moments) depend upon the dimensionless time step, Δt^*, number of particles, N, and the number of trials, L. In this particular case, since it is a single event with a fixed characteristic time, τ, there is no error due to the dimensionless splitting time step Δt^*. *With $\Delta t^* > 1$, algorithm 3 is implemented*, as algorithm 2 can be implemented only up to $\Delta t^* = 1$. We study the order of convergence with respect to N, with $\Delta t^* = 4/3$.

Inflow as uniform distribution: The order of convergence is studied in the regime where the systematic error is greater than the statistical error. The error with respect to the number of particles N is displayed in **Table** 1.

Table 1: *Computational study for varying N (moment* 1*, inflow as uniform distribution)*

	Algorithm 1		**Algorithm 3**	
N	$c_{tot} \times 10^4$	$c_{stats} \times 10^4$	$c_{tot} \times 10^4$	$c_{stats} \times 10^4$
26	115.970	4.805	115.575	4.760
50	60.232	4.876	60.293	4.900
100	29.990	4.898	30.083	4.900
200	10.589	4.988	15.035	5.000
400	7.589	5.007	7.520	4.860
800	4.541	5.101	3.954	4.670
1600	3.045	4.966	2.307	5.000
3200	1.237	4.771	2.030	4.192
6400	1.050	5.500	1.400	5.000

With increase in the value of N, the systematic error reduces and the statistical error bounds of the numerical solution encompass the analytical solution. **Figure** 4 shows the order of convergence for moment 1, for algorithm 1 and algorithm 3, with the inflow as delta distribution. The error bars denote the statistical error. ***Figure** 4 suggests convergence of order N^{-1} for both the algorithms.*

Inflow as delta distribution: With the inflow as delta distribution, **Figure** 5 gives the systematic and statistical errors with respect to N. As observed for inflow as a uniform distribution the results suggest an order N^{-1} in this case as well.

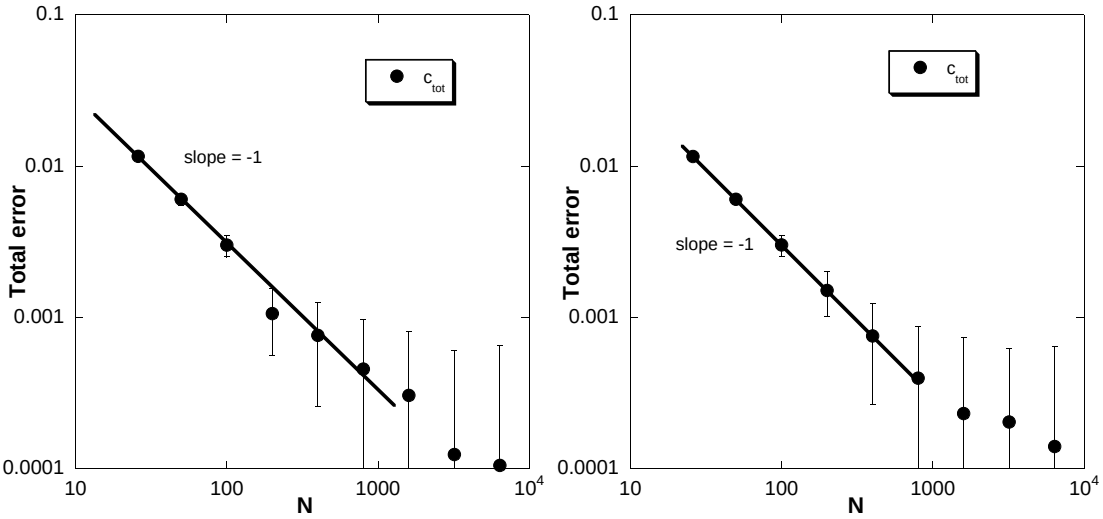

(a) Algorithm 1 (b) Algorithm 3

Figure 4: *Order of convergence for* ***Table*** *1*

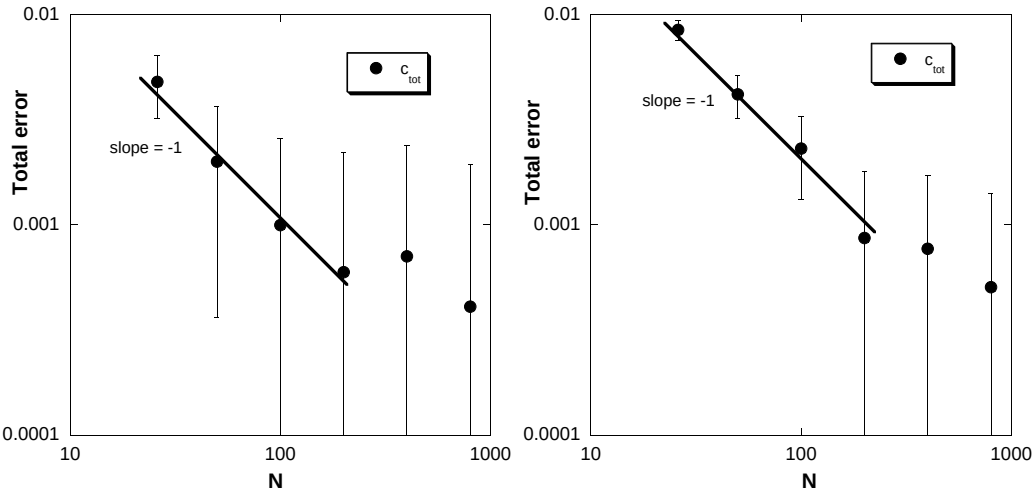

(a) Algorithm 1 (b) Algorithm 3

Figure 5: *Order of convergence for inflow-outflow (inflow: delta distribution)*

4.2.2 Inflow-Outflow + Mixing + Reaction

Here we consider inflow-outflow, mixing and reaction events with two subcases: one where all three characteristic times are of the same order of magnitude, and

Table 2: *Computational study for varying N (moment 2, inflow as uniform distribution)*

	Algorithm 1		**Algorithm 2**	
N	$c_{tot} \times 10^4$	$c_{stats} \times 10^4$	$c_{tot} \times 10^4$	$c_{stats} \times 10^4$
26	11.400	3.600	383.250	0.00008
50	6.000	3.710	383.250	0.00008
98	3.600	3.760	383.250	0.00008
196	3.549	3.770	383.250	0.00008
390	3.061	3.800	383.250	0.00008
782	2.980	3.900	383.250	0.00008
1562	2.990	3.980	383.250	0.00008
3126	2.756	4.000	3.139	3.100
6250	2.766	4.200	3.107	3.105
12500	2.758	4.220	3.000	3.200

the second, where the characteristic time for inflow-outflow is much lower than the characteristic times for mixing and reaction.

For the *first subcase*, the characteristic times for these events are set as given in Section 4.2.1. The product $N \times L = 750000$ is kept fixed. *From the error study in section 4.1, the error obtained at* $\Delta t^* = 0.001$ *is comparable to the statistical fluctuations obtained in the particle method and hence* Δt^* *is fixed at* 0.001 . As described earlier, at such low values of Δt^*, algorithms 2 and 3 are identical. We investigate the error with respect to the number of particles, N, for algorithm 1 and algorithm 2. **Table** 2 shows the systematic and statistical errors with respect to N for the second moment, with inflow condition as a uniform distribution.

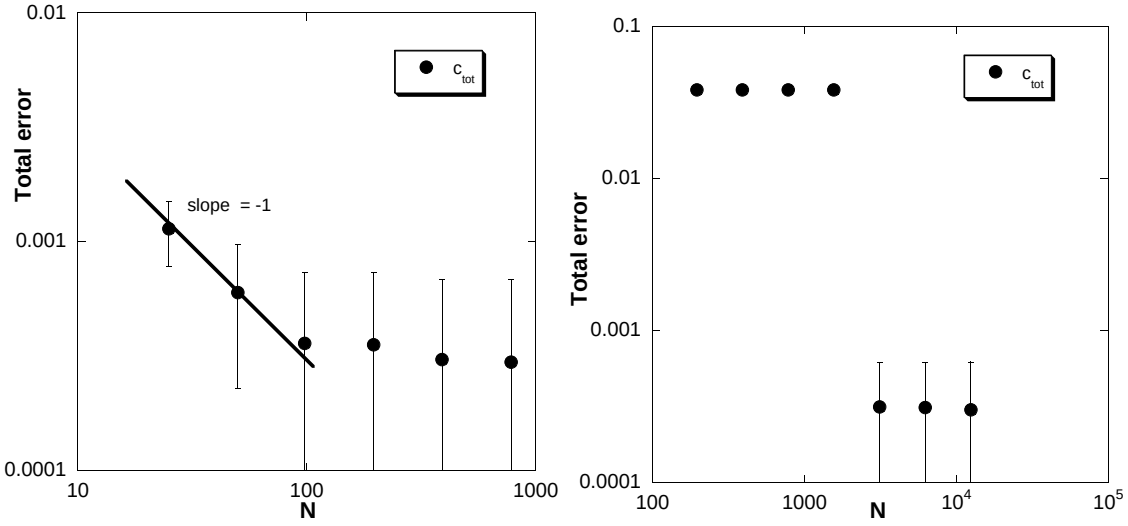

(a) Algorithm 1

(b) Algorithm 2

Figure 6: *Order of convergence for* ***Table*** *2*

Figure 6 shows the systematic error with respect to N, for inflow as uniform distribution. For the case of algorithm 2, the number of inflow particles to be replaced, N_{in}, is calculated according to Equation (3.3.2). As algorithm 2 considers a mean waiting time parameter of the stochastic process, it requires a certain minimum number of particles, N, in order to let at least one particle be replaced and thus allow the inflow-outflow event to occur. Therefore at the value of Δt^* implemented, it needs approximately $N = 3000$, so that the inflow-outflow event occurs. However for algorithm 1, with L trials, the inflow-outflow event can occur at a lower value of N, as depicted in **Figure** 6(a). Similar results are obtained for second and third moments for both the conditions of inflow.

Thus, *algorithm* 1*, based on a stochastic jump process can be implemented at low values of* N*, at the expense of a greater number of repetitions.*

For the *second subcase*, the characteristic time for mixing is set to $\tau_m = 5000$, and that for the reaction is $\tau_r = 5000$. The residence time is 3.0, and the dimensionless time step $\Delta t^* = \frac{\Delta t}{\tau} = \frac{4}{3}$. With $\Delta t^* > 1$, algorithm 1 and algorithm 3 are compared. **Table** 3 gives the systematic and statistical errors for the first moment with inflow as delta distribution. As shown in **Figure** 7, the order of convergence obtained with both the algorithms is the same, thus the *systematic error scales as* N^{-1}.

Table 3: *Computational study for varying N (moment 2, inflow as delta distribution)*

	Algorithm 1		**Algorithm 3**	
N	$c_{tot} \times 10^4$	$c_{stats} \times 10^4$	$c_{tot} \times 10^4$	$c_{stats} \times 10^4$
50	25.000	8.000	41.232	5.003
100	14.000	8.200	20.783	4.990
200	9.590	8.000	9.542	4.990
400	6.970	8.000	6.997	5.000
800	6.400	8.200	5.689	5.100
1600	5.000	8.000	5.000	5.300
3200	4.600	8.000	4.600	3.100
6400	4.510	8.200	4.500	5.220
12800	4.500	8.000	4.500	5.300

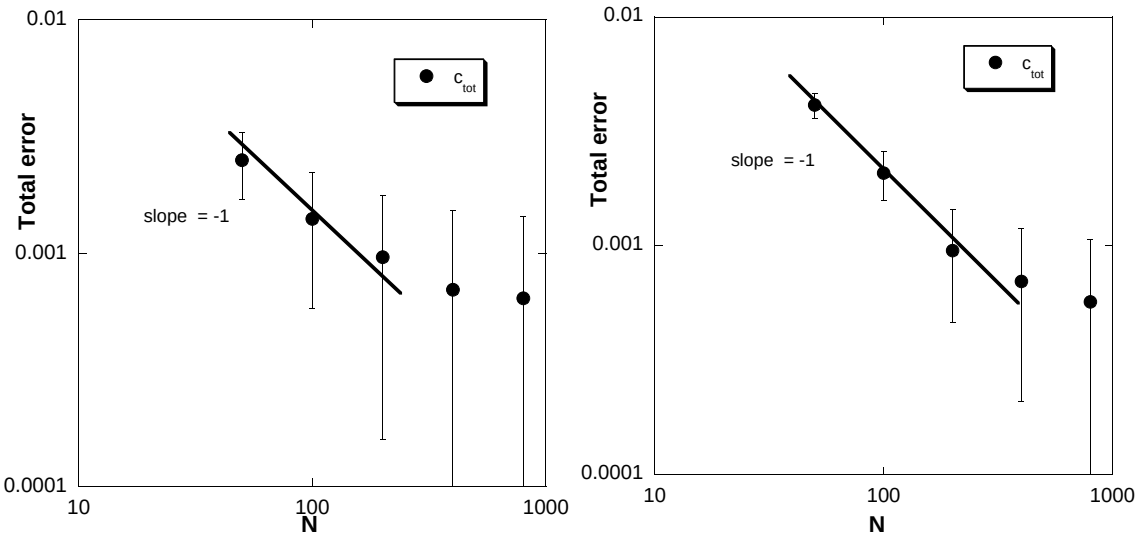

(a) Algorithm 1

(b) Algorithm 3

Figure 7: *Order of convergence for* ***Table*** *3*

Similar results are obtained for the second and third moments for both the inflow conditions. With $\Delta t^* > 1$, even small number of particles (say$100 - 200$) are sufficient to let the inflow-outflow event occur, contrary to the earlier subcase where $\Delta t^* = 0.001$ (**Figure** 6). The CPU time is proportional to the non-dimensional time splitting step. Adopting *algorithm* 3 enables the use of *larger time steps* as compared to algorithm 2, thus *saving computational expense* in terms of CPU time.

5 Combustion of kerosene

In this section, the PaSR model is applied to a practical combustion case: premixed kerosene-air combustion.
Case study: A premixed kerosene-air stream flows into a reactor at a high flow rate (small residence time, $\tau = \tau_1$). With very small residence time, the kerosene-air mixture fails to ignite. After the steady state is reached, the flow rate of the inflow stream is reduced resulting in a large enough residence time ($\tau = \tau_2$) and ignition of the kerosene-air mixture.

5.1 Implementation of PaSR model

In the *first part* the time step can be set greater than τ_1, as shown in Section 4.2.2. Hence the inflow-outflow event is modelled by implementing algorithm 3. In addition the inflow-outflow event is modelled using algorithm 2, and the CPU times consumed by each algorithm are compared. In the *second part* the ratio of $\frac{\Delta t}{\tau_2}$ should be chosen to be much less than unity, as described in Section 4.2.2. At a low value of $\frac{\Delta t}{\tau_2}$, algorithms 2 and 3 are identical. The combustion chemistry is modelled by a reaction mechanism comprising of 57 chemical species and 273 chemical reactions [3]. The initial conditions for the concentrations are: $X_{n-C_{12}H_{26}} = 6.624 \times 10^{-3}, X_{O_2} = 2.086 \times 10^{-1}$ and $X_{N_2} = 7.848 \times 10^{-1}$ with the concentration of the remaining 54 species being zero. The inflow stream has the same composition as mentioned above. The chemical kinetics are computed with the Chemkin-III [9] package and the stiff chemical kinetics are solved using the Senkin package [14]. The air/fuel ratio = 25.4 and the pressure is kept constant at 1.5133×10^6Pa. The other numerical parameters are given in **Table** 4.

Table 4: *Numerical parameters for part one and part two*

Quantity	**part one**	**part two**
τ	$1 \times 10^{-2}\mu\mathbf{s}$	$4 \times 10^{-3}\mathbf{s}$
T_{inflow}	$2000\mathbf{K}$	$1000\mathbf{K}$
$T(0)$	$1200\mathbf{K}$	$2000\mathbf{K}$
τ_m	$1 \times 10^{-4}\mathbf{s}$	$1 \times 10^{-4}\mathbf{s}$

5.2 Results of the modelling study

In part one, no ignition occurs. The temperature evolution is shown in **Figure** 8.

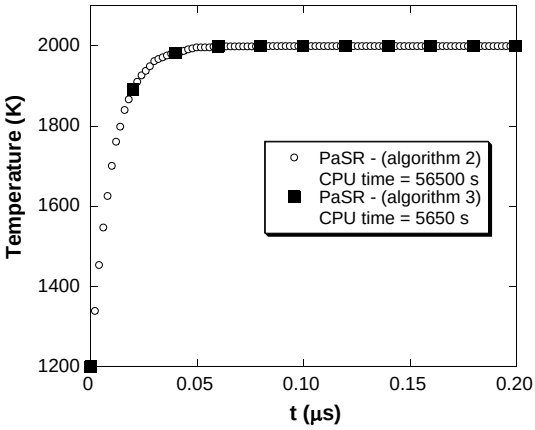

Figure 8: *Comparison of the temperature evolution obtained with algorithm* 2 *and algorithm* 3

The non-dimensional time step $\Delta t^* = \frac{\Delta t}{\tau}$ is 0.2 for algorithm 2 and 2.0 for algorithm 2. The CPU time consumed by algorithm 2 is an order of magnitude greater than that consumed by algorithm 3.

In part two, the ignition occurs and the temperature increases rapidly and then settles down to a steady state at 2200K as shown in **Figure** 9(a). **Figure** 9(b) depicts the NO_X and CO emissions from the combustion in part two.

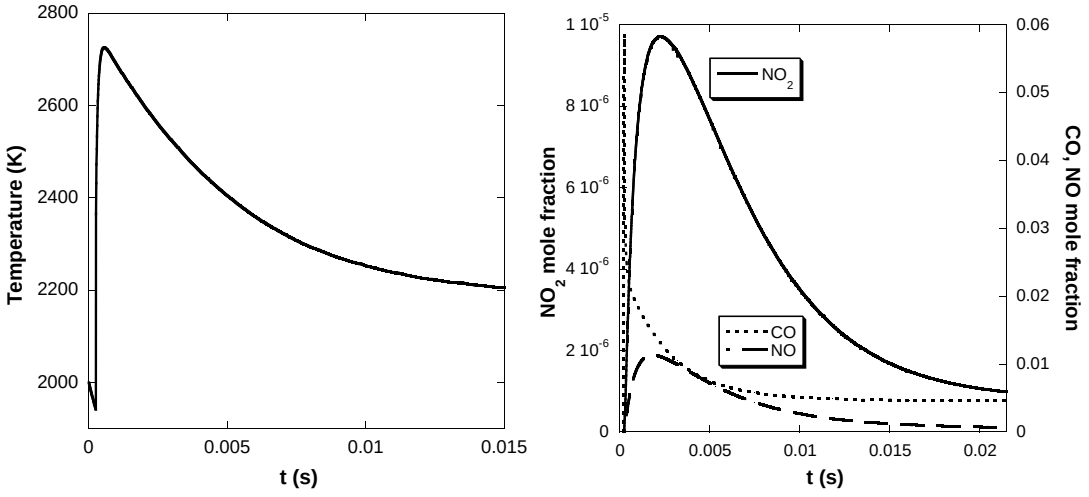

(a) Temperature profile for part two

(b) CO and NO_X emissions for part two

Figure 9: *Temperature profile and emissions:* $N = 1000$ *and* $1 \times 10^{-5} s$

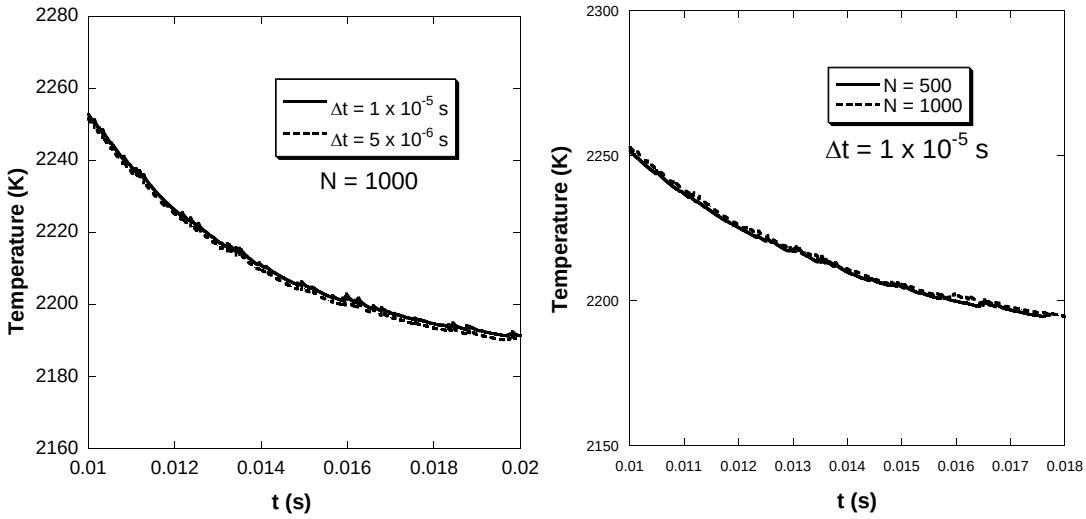

(a) varying Δt (b) varying N

Figure 10: *Steady state*

Convergence with respect to N and Δt was studied for two time regimes; steady state (as shown in **Figure** 10) and transient state (**Figure** 11). The convergence study for the steady state regime indicated that the parameters $N = 1000$ and $\Delta t = 5 \times 10^{-6} s$, gave a 0.1% error.

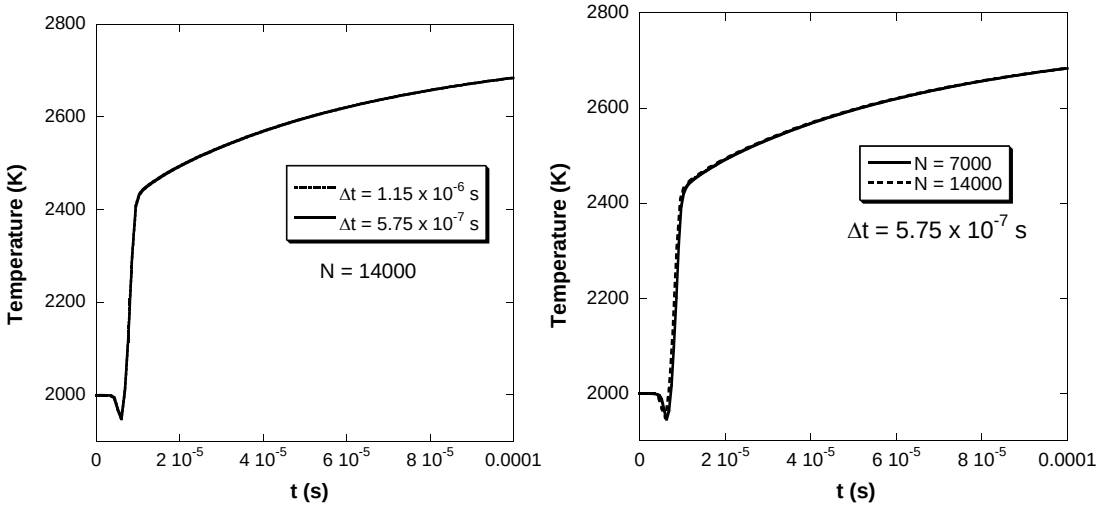

(a) varying Δt (b) varying N

Figure 11: *Transient state*

The ignition delay as given by the PaSR simulation depends upon the size of the time step. In the transient state, $\Delta t = 1.15 \times 10^{-6} s$ and $N = 7000$ were sufficient to yield an error of 1%.

6 Conclusion

In this paper we presented a detailed numerical investigation of the partially stirred reactor (PaSR) model. The need for such a numerical study was motivated by the dearth of analytical solutions for the PDF based methods, and by the problems mentioned in the literature regarding the size of time step in a Monte Carlo particle method with time splitting algorithm, applied to PaSR.

Analytical solutions were developed for the first four moments of the mass density function (MDF) obtained from the PaSR model. On the basis of the analytical solutions developed an inflow-outflow algorithm was derived (algorithm 3). It was demonstrated that the algorithm mentioned in the literature (algorithm 2) is a special case (for the condition $\frac{\Delta t}{\tau} < 1$) of the more general algorithm 3. An inflow-outflow algorithm (algorithm 1) based on a stochastic jump approach was also presented. Algorithm 2 was explained by considering a deterministic parameter of the waiting time in the algorithm 1.

The analytical solutions for the moments were split according to first order splitting and the splitting error scales as Δt^*(ratio of time step to the characteristic time of an event). On implementing the Monte Carlo particle method with time splitting, the convergence studies suggest that the systematic error is inversely proportional to the number of particles, N.

The three inflow-outflow algorithms were implemented in the Monte Carlo particle method. As compared to algorithms 2 and 3, the algorithm 1 requires a fewer particles N, but at the expense of L simulation trials. From the model reaction $A \longrightarrow B$ and the combustion of kerosene studies, it can be concluded that the non dimensionless time step Δt^* must be less than unity when the characteristic times for inflow-outflow, reaction and mixing are of comparable order of magnitude. However, with the residence time very small compared to the characteristic times for reaction and mixing, algorithm 3 can be employed with the condition $\frac{\Delta t}{\tau} > 1$ and is an order of magnitude faster than algorithm 2, thus saving the computational expense.

7 Acknowledgements

Financial support from the Cambridge Commonwealth trust and the ORS committee is gratefully acknowledged. The authors thank Mike Goodson, Uri Zarfaty (University of Cambridge) and Wolfgang Wagner (Weierstrass Institute for Applied Analysis and Stochastics, Germany) for their mathematical expertise and help.

References

[1] Bendat, J. S. and Piersol, A. G. (1971). *Random Data: Analysis and measurement procedures*, 1st edn, Wiley-Interscience, pp. 99–129.

[2] Bender, R., Blasenbrey, T. and Maas, U. (2000). Coupling of detailed and ILDM reduced chemistry, *Proc. Comb. Inst.* **28**: 101–106.

[3] Brite-Euram (1999). Final report: Pdf/cfd-based methods: Development and validation for low emission combustor technology.

[4] Cannon, S. M., Brewster, B. S. and Smoot, L. D. (1998). Stochastic modeling of CO and NO in premixed methane combustion, *Combustion and Flame* **113**: 135–146.

[5] Chen, J. Y. (1997). Stochastic modeling of partially stirred reactors, *Combust. Sci. and Tech.* **122**: 63–94.

[6] Correa, S. M. and Braaten, M. E. (1993). Parallel simulations of partially stirred methane combustion, *Combustion and Flame* **94**: 469–486.

[7] Eibeck, A. and Wagner, W. (2000). An efficient stochastic algorithm for studying coagulation dynamics and gelation phenomena, *SIAM J. SCI. COMPUT.* **22**(3): 802–821.

[8] Hammersley, J. M. and Handscomb, D. C. (1964). *Monte Carlo Methods*, 1st edn, London: Metheuen and Co. Ltd., pp. 1–96.

[9] Kee, R. J., Rupley, F. M., Meeks, E. and Miller, J. A. (1996). Chemkin-III: A fortran chemical kinetics package for the analysis of gas phase chemical and plasma kinetics. technical report, sandia report sand 96-8216 uc405.

[10] Kraft, M. (1998). *Stochastic Modelling of Turbulent Reacting Flow in Chemical Engineering*, number 391 in *Fortschrittsberichte des VDI, Reihe 6*, 1st edn, Dusseldorf: VDI Verlag, pp. 30–203.

[11] Kraft, M. and Fey, H. (1999). Some analytic solutions for stochastic reactor models based on the joint composition PDF, *Combust. Theor. Model.* **3**(2): 343–358.

[12] Kraft, M. and Wagner, W. (2000). Numerical study of a stochastic particle method for homogeneous gas phase reactions, *WIAS Preprint Series* **570**: 1–27.

[13] Levenspiel, O. and Spielman, L. A. (1965). Monte Carlo treatment for reacting and coalescing dispersed phase systems, *Chem. Engng. Sci.* **20**: 247–254.

[14] Lutz, A. E., Kee, R. J. and Miller, J. A. (1988). Senkin: A Fortran program for predicting homogeneous gas phase chemical kinetics with sensitivity analysis. technical report, sandia report sand 87-8248 uc401.

[15] Nooren, P. A., Wouters, H. A., Peeters, T. W. J., Roekaerts, D., Maas, U. and Schmidt, D. (1997). Monte Carlo pdf modelling of a turbulent natural gas diffusuion flame, *Combust. Theory and Modelling* **21**: 79–96.

[16] Pope, S. B. (1981). A monte carlo method for the pdf equations of turbulent reactive flow, *Combust. Sci. Technol.* **25**: 159–174.

[17] Pope, S. B. (1985). Pdf methods for turbulent reactive flows, *Energy Combust. Sci.* **11**: 119–192.

[18] Sabelnikov, V. and Da Silva, L. F. F. (2002). Partially stirred reactor: Study of the sensitivity of the Monte Carlo simulation to the number of stochastic particles with the use of a semi-analytic, steady-state solution to the PDF equation, *Combustion and Flame* **129**: 164–178.

[19] Xu, J. and Pope, S. B. (1999). Assessment of numerical accuracy of pdf/monte carlo methods for turbulent reactive flows, *J. Comput. Phys.* **152**: 193–230.